Soil and Climate Factors Drive Spatio-temporal Variability of Arable Crop Yields under Uniform Management in Northern Italy

Abid Ali[a], Roberta Martelli [a]*, Elia Scudiero[b], Flavio Lupia[c], Gloria Falsone[a], Valda Rondelli[a] and Lorenzo Barbanti[a]

[a]*Department of Agricultural and Food Sciences, University of Bologna, Viale Fanin 50, 40127 Bologna, Italy;* [b]*Department of Environmental Sciences, University of California, Riverside, 450 West Big Springs Road, Riverside, 92507, California, USA;*[c]*CREA Research Centre for Agricultural Policies and Bioeconomy, via Po, 14, 00198 Rome, Italy.*

**Correspondence: roberta.martelli@unibo.it*

Soil and Climate Factors Drive Spatio-temporal Variability of Arable Crop Yields under Uniform Management in Northern Italy

Soil and weather data were used to analyse spatio-temporal yield patterns of winter cereals (wheat) and spring dicots (sunflower and coriander) in a 11-ha field in Northern Italy (44.5° N, 12.2° E), during 2010-2014. Three yield stability classes (YSCs) were established over multiple years, based on spatio-temporal characteristics across the field: high yielding and stable (HYS), low yielding and stable (LYS), and unstable. The HYS class (46% of field area) staged a 122% relative yield with low temporal variability. The unstable class (24% of field area) was slightly more productive (83% relative yield) than the LYS class (30% of field area, and 80% relative yield), but less consistent over time. Crop yields evidenced negative correlations with sand content; positive correlations with silt and clay content. Soil properties were quite consistently classified among YSCs: the LYS and unstable classes were associated with higher sand content and lower cation exchange capacity, suggesting that these characteristics lead to fluctuation and depression of final yield. Establishing YSCs based on spatio-temporal yield appears a sound approach to appraise field potential. It results in strategic and tactical decisions to be taken, depending on the profile of spatial and temporal productivity in different field areas.

Keywords: Apparent soil electrical conductivity; crop yield; field spatio-temporal variability; geostatistics; soil properties

Introduction

Precision agriculture (PA) has a great potential to increase crop growth and final yield through the application of variable crop inputs (Basso et al. 2017). Specific crop inputs at the right time and place is highly encouraged in today's agriculture. Therefore, the focus of this study is to analyse spatial and temporal variability of field crops, in-season climate conditions, and soil nutrient status for optimizing crop productivity and sustaining the most efficient use of finite natural resources (Blackmore 2000; Maestrini and Basso 2018). Soil physical-chemical properties vary in space and time depending on their interaction with factors such as climate, topography and anthropogenic activities (Corwin et al. 2003). Bullock and Bullock (2000) stressed the importance of adopting efficient methods to characterize soil spatial variability. Among them, apparent soil electrical conductivity (ECa) directed to soil sampling has been shown a rapid and reliable method to characterize field variability (Corwin and Lesch 2003). However, ECa has not always staged consistent results with crop yield, due to its complex interactions with soil properties and external factors (Corwin et al. 2003).

Climatic factors exert a strong influence on crop productivity under rainfed conditions (Iizumi and Ramankutty 2015; Asfaw et al. 2018), being responsible for consistently low yielding areas where insufficient moisture is the most limiting factor. Several studies demonstrate that the two main climatic factors, precipitation and temperature, significantly influence yield stability across growing seasons (Kukal and Irmak 2018; Maestrini and Basso, 2018; Mohsenipour et al. 2018; Shiru et al. 2018). Precipitation is seen to be more impacting than the temperature on final crop yield (Kang et al. 2009)

During the 21st century, it is expected that higher temperatures influence the regime of precipitation, and the ultimate availability of water (Mishra et al. 2014). Therefore, registering the weather course during the crop season stimulates farmers to think critically regarding crop management (Cuculeanu et al. 2002; Asfaw et al. 2018).

Furthermore, biotic and abiotic factors equally contribute to influence crop growth and development, and final yield. Among abiotic factors, low water availability and heat exert an influence on final crop yield (Mariani and Ferrante 2017), also depending on genotype adaptation to specific adversities (Zandalinas et al. 2018).

In this complex situation, many studies addressed different methods of delineating site-specific crop management (SSCM) zones within a field, by relating yield data with soil properties and external factors. Da Silva (2006) produced classified zones based on spatio-temporal yield maps. Lark and Stafford (1996) used an unsupervised fuzzy clustering method over multiple years' yield data. Swindell (1997) analyzed the spatial variability by using several crop harvest indices. Fraisse et al. (1999) combined topographical variables and ECa through unsupervised cluster analysis. Maestrini and Basso (2018) produced zones based on spatio-temporal yield of several crops with soil, crop reflectance and weather data during the growing seasons.

This research was aimed at identifying homogeneous areas for site-specific management, using soil and crop yield data. The following steps were carried out: i) establishment of spatio-temporal yield stability classes (YSCs) (Blackmore, 2000; Panneton and Brouillard 2002; Blackmore et al. 2003), based on the yield data of a five-year crop rotation under uniform, rainfed management; ii) assessment of the spatial variability of soil properties determined in samples taken according to an ECa; iii) establishment of spatio-temporal YSCs based on soil properties; iv) analysis of the weather effects on temporal yield variability in the five crop seasons.

Materials and Methods

Study site description

The experimental site was an 11.07-ha field of the Agrisfera Cooperative, located near Ravenna, Italy, at N 44° 29' 26", E 12° 07' 44", 0 m above sea level (Figure S1). The area falls in the Mediterranean North Environmental Zone (Metzger et al. 2005). The field was managed in a uniform rotation system with winter cereals Durum Wheat in 2010 (DW 2010) and Bread Wheat in 2012 and 2014 (BW 2012 and 2014), and spring dicots, Sunflower in 2011 (SF 2011) and Coriander in 2013 (CO 2013). Cultivation was based on the good practices for each specific crop, depending on the local conditions. The previous field history from 1976 to 2005 (Figure S2) shows three separate parts of approximately equal length (200 m each in the north-south axis), cultivated with fruit orchard and vineyard (upper, i.e. northern, part), and arable crops (lower, i.e., southern, part). In 2006, the three fields were merged into a single arable field (Figure S2).

Crop data management

Five years' georeferenced grain yield (GY) data was collected by a New Holland CR 9080 (CNH Industrial N.V., Basildon, UK), equipped with an assisted guiding system based on real-time kinematic GPS, yield mapping system consisting of a Pektron flow meter (Pektron Group Ltd, Derby, UK), and Ag Leader moisture sensor (Ag Leader Technology, Ames, IA, USA).

Raw yield data were processed and filtered using Yield Editor software (Version 2.0.7; USDA-ARS Cropping Systems and Water Quality Research, Columbia, Missouri). An average of 6170 GY data points per crop were retained in the experimental area. The sowing and harvesting dates were: DW 2010, Oct. 30 (2009) – Jul. 10; SF 2011, Apr. 5 – Sep. 7; BW 2012, Oct. 14 (2011) – Jul. 1; CO 2013, Apr. 11 – Jul. 10; BW 2014, Nov. 9 (2013) – Jul. 7.

Thereafter, a geostatistical analysis was performed on GY data to i) examine the degree of spatial dependence (SpD) in terms of semivariogram; ii) produce continuous grid points over the entire field before mapping; iii) combine the interpolated data intersected on the regular grid. Three main parameters describe semivariogram characteristics: i) nugget (C_0), the measurement error at 0 distance (h=0); ii) sill (C_0 + C), the maximum y-axis value that increases with increasing lag distance (h), and remains constant at a higher distance; iii) range (a), the maximum distance at which data points are still correlated, i.e. the lag distance at sill value. The degree of SpD as given by Cambardella et al. (1994) explains the nugget to sill ratio ($C_0/(C_0 + C)$): < 25 %, indicates strong SpD; (ii) 25-75 %, moderate SpD; (iii) >75 %, weak SpD.

We employed the iterative cross-validation technique seeking the highest coefficient of determination (R^2) and minimum mean absolute error (MAE) to choose the best fitting semivariogram model among Circular, Spherical, Exponential, Gaussian, and Stable (Xiao et al. 2016). Spatial variability maps were computed by simple kriging (SK) with 10 m cell size, resulting in 24 columns and 72 rows (Moral et al. 2010; Ali et al. 2019). SK was chosen as it provides, normally, maximum R^2 and minimal error parameters (Xiao et al. 2016).

For each crop, standardized interpolated data with 1156 regular grid points were used for comparison among years, by replacing the actual GY (t/ha) with a relative GY where 100 % equals field average. This allowed data from different crops to be jointly analyzed. The Equation (1) was used to characterize the spatial variability maps over a single crop:

$$S_i = \left(\frac{y_i}{\bar{y}}\right) \times 100 \quad (1)$$

Where, S_i=standardized yield (%) over 100 % field average at point (i), y_i=interpolated yield at point i (t/ha), and $\bar{y}$=mean interpolated yield over the entire field (t/ha).

For multiple crops, a spatial variability map was produced by simply calculating the mean standardized yield, laid over the five years according to Equation (2).

$$\bar{S}_i = \frac{\sum_{t=1}^{n} S\, i_I}{n} \quad (2)$$

Where, $\bar{S}_i$= mean interpolated yield over 100% field average over n years, Si_I= interpolated standardized yield (%) at point (i).

For multiple crops, a temporal variability map was produced to assess the stability of standardized GY over the five crop years. The coefficient of variation (CV) of each grid point over the five years was calculated based on Equation (3) (Blackmore 2000).

$$CVS_i = \frac{\left(\frac{\left(n \sum_{t=1}^{t=n} Si_t^{\ 2} - (\sum_{t=1}^{t=n} Si_t)^2\right)}{n(n-1)}\right)^{0.5}}{\bar{S_\iota}} \times 100 \quad (3)$$

Where, CVS_i= coefficient of variation of standardized yield at point *(i)* over *n* years; Si_t = standardized yield (%), at point *(i)*; $\bar{S_\iota}$ = mean standardized yield at point *(i).*

To define the threshold levels in spatial maps, four classes were established in both single- and multiple-year yield, based on the natural break classification method (Toshiro 2002): very low (VL), medium-low (ML), medium-high (MH) and very high (VH). Each class showed maximum difference with other classes, while the within-class variability was minimized. Likewise, four classes were defined for temporal variability map across CV ranges between 2% and 73%.

Spatio-temporal yield variability analyses

Three yield stability classes (YSCs) were produced by combining the spatial and temporal maps over multiple crops (Table S1): high yielding and stable (HYS) ($\bar{S}_i$>100, CV_{Si}<30), low yielding and stable (LYS) ($\bar{S}_i$<100, CV_{Si}<30), and unstable (CV_{Si}>30). Each class was derived from spatio-temporal yield data of multiple crops (equations 2 and 3), by applying the combinational logic statement (Blackmore 2000).

Soil sampling

The positions for soil samples were based on the procedure developed by Corwin and Lesch (2005). First, a soil ECa survey was conducted using an on-the-go sensor CMD Tiny Electromagnetic Conductivity Meter (GF Instruments, s.r.o., Brno, Czech Republic) along a 8 m transect over the field area (Figure 1), removing outliers from raw ECa values, which left a total of 2651 data points (Figure 1). Then, the ECa-directed Response Surface Sampling Design module in ESAP-95 version 2.01 (Lesch et al. 2000) was used to delineate the scheme for 20 soil samples to be taken (Figure 1). Soil cores were taken at the 0-30 and 30-60 cm soil depth. The samples were air-dried at 40 °C and sieved at 2 mm diameter.

Figure **1**

Soil physico-chemical analysis, and spatial variability

The twenty soil samples (200-250 g) at 0-30 and 30-60 cm depth were subjected to determination of the following properties: particle size distribution (sand, silt, and clay content), pH, total carbonates ($CaCO_3$), total organic carbon (C), total nitrogen (N), available P (P Olsen), exchangeable cations (K, Ca, Mg, Na), cation exchange capacity (CEC), and electrical conductivity of a soil extract with a 1:2.5 (w/w) soil-to-water ratio ($EC_{1:2.5}$). The particle size distribution was determined by the pipette method (Gee and Bauder 1986). Soil pH was measured at 1:2.5 (w/w) soil-to-water ratio. The total carbonate content ($CaCO_3$) was volumetrically determined (Loeppert and Suarez 1996). Total organic C and total N concentrations were determined by a CHN elemental analyzer (EA 1110 Thermo Fisher, Waltham, MA, USA). The available P was extracted according to Olsen et al. (1954) and was measured by inductively coupled plasma optical emission spectrometer (ICP-OES, Ametek, Spectro Arcos, Kleve, Germany). The cation exchange capacity (CEC) and the exchangeable cations were determined according to the method proposed by Orsini and Rémy (1976) and modified by Ciesielski and Sterckeman (1997), and the amounts of Co and exchangeable cations were measured by ICP-OES. Soil electrical conductivity (EC) was determined on 1:2.5 (w/w) soil-to-water ratio aqueous suspension and then reported as EC on the saturation extract (ECe).

For soil spatial variability, we produced the maps of soil properties in the 0-60 cm soil depth (average of the 0-30 and 30-60 cm layers), by using ordinary kriging with 10 m grid resolution. Kriging outperforms normally the inverse-distance weighted method in spatial soil mapping (Kravchenko and Bullock 1999; Reza et al. 2010; Daniel et al. 2017).

Relationship between spatio-temporal YSCs and soil data

Thirty m wide buffers around the 20 positions determined by the ESAP software were created for statistical correlations between spatio-temporal yield and soil properties. The values of interpolated GY and selected soil properties falling within the range of each buffer were averaged for Pearson's correlations (*r*) involving the 20 data points. Thereafter, it was evaluated if multi-years spatio-temporal yield could effectively be described by the differences in soil properties within YSCs. To this aim, interpolated soil data were associated with the YSCs, then the statistical differences of soil properties among YSCs were assessed in the same way as described by Li et al. (2008) and Scudiero et al. (2018).

The weather information during the five growing seasons (Hydro-meteorological Service of the Emilia-Romagna region) was used to interpret temporal yield variability. The wet and dry periods from initial to maturity stages of the surveyed crops were represented by the balance between precipitation (P) and crop evapotranspiration (ET_C), this latter determined according to Allen et al. (1998). In the supplementary materials, total precipitation and the average temperature were computed monthly according to Bagnouls and Gaussen (1953), to indicate wet and dry periods during the five crop seasons.

Map production and geostatistical data analysis were carried out with the ArcGIS software (Version 10.3, ESRI, Redlands, CA, USA) under the reference system WGS 84/UTM zone 32 °N. Statistical analyses were performed with the Statistica 10 software (StatSoft Corp., Tulsa, OK, USA).

Statistical analysis

Crop yields and soil data were subjected to descriptive statistics. Pearson's correlation (r) was used to evaluate the relationships of soil properties and spatio-temporal relative yield in single and multiple crops. One way analysis of variance (ANOVA) was run to assess the differences in soil and yield traits among the three YSCs. The least significant difference (LSD) at $P \leq 0.05$ was used to indicate significantly different levels.

Results

Descriptive statistics of crop yields

Table 1a summarizes the characteristics (mean, minimum, maximum, SD, kurtosis, and skewness) of standardized GY data in the five years. Crop yield varied greatly across the field. The widest min.-max. range (183) was found in BW 2012, whereas the tightest range (143) was shown in DW 2010. Standardized GY variability was generally high, as indicated by SD ranging from 29 % for DW 2010 to 38 % (SF 2011 and CO 2013).

Table **1**

Geostatistics of crop yields

The spatial patterns of crop yields were evaluated in terms of semivariograms and the respective model fittings (Table 1b). DW 2014 showed a zero nugget effect, followed by SF 2011 and DW 2010 with very low nugget values. All crops exhibited a quite similar total variance (sill variance

(C_0+C) ranging from 0.92 to 1.17), whereas the range (a) varied noticeably between 38 and 121 m. A high/low range indicates high/low continuity, respectively, within the dataset. Based on the degree of SpD (Cambardella et al. 1994), crop data showed a 'strong' continuity in their SpD in all cases except BW 2012. The results of semivariogram model fitting (R^2 and MAE) confirmed the good performance of the stable and exponential variogram, depending on years, over the empirical data (Xiao et al. 2016; Bhunia et al. 2018).

Yield maps and spatio-temporal variability

Spatial maps of standardized GY were traced depicting the four yield classes in the fivee years (Figure 2a, 2b, 2c, 2d, 2e). Spatial variability map over multiple crops (Figure 2f) exhibited higher minimum (27) and lower maximum (148) relative GY, resulting in a narrower range (121) compared to single crops. Nevertheless, spatial variability maps in single vs. multiple crops were quite consistent, i.e. areas at high or low GY tended to repeat in the same position. The upper field portion (4.12 ha) always showed low and below-average yield, whereas the middle and lower field portions (6.95 ha) always featured above average and high yield.

In the spatial map over multiple crops (Figure 2f), an area of 1.30 ha (11.7 % of the field surface) lay in the VL area, 3.86 ha (34.8 %) in the ML area, 3.10 ha (28.1 %) in the MH area, and 2.81 ha (25.4 %) in the VH area. In the temporal map (Figure 2g), high stability (CV up to 30 %) covered an area of 8.27 ha (76 %) across the field, while the unstable area (CV = 30-73 %) covered the remaining 2.8 ha (24 %) (Figure 2g). Lastly, the three yield stability classes (HYS, LYS and unstable) depicted the features of spatio-temporal yield over multiple years (Figure 2h).

Figure **2**

Yield data distribution within spatio-temporal yield stability classes

Data distribution within the classes of spatio-temporal maps is reported in Table 2.

Table **2**

For spatial variability classes, in DW 2010 GY data distribution was more skewed towards high yielding classes, meaning that more grid points belonged to the MH and VH classes. The same occurred, to a lesser extent, in all the other years except SF 2011. Also the multiple crops combined showed a slight prevalence of the MH and VH classes. The differences between the relative GY values in single and multiple crop maps indicate that class limits and width are not the same between single and multiple datasets.

For temporal variability classes, 334 data points out of 1156 (28.9 % or 3.3 ha) were in the highly stable class (2-14 % CV), 310 points (26.8 % or 3.1 ha) were in the medium stable class (14-22 % CV), 235 points (20.3 % or 2.4 ha) in the lowly stable class (22-30 % CV), and finally 277 data points (24 % or 2.8 ha) were in the unstable class (30-73 % CV).

For yield stability classes, 527 data points (46 % or 5.3 ha) were found in the HYS class, 352 (30 % or 3.5 ha) in the LYS class, and 277 points (24 % or 2.8 ha) in the unstable class.

Spatial variability of soil properties

The descriptive analysis of soil physico-chemical properties in the average of the two depths (0-60 cm) is reported in the supplementary material (Table S2). The soil was loamy, moderately alkaline, rich in carbonates, poor of organic carbon (< 10 g/kg), and with a low C:N ratio (< 10). Available P and exchangeable K were also quite low (< 10 mg/kg and < 0.3 $cmol_+$/kg, respectively). Exchangeable Ca was relatively high (almost 80% of the CEC). ECe denoted a negligible salinity across the field. Lastly, the three particle size classes (sand, silt, and clay) were more heterogeneous (higher SD in proportion to mean data) than the rest of the soil properties.

Spatial soil maps

Spatial maps of soil properties interpolated with ordinary kriging are reported in Figures 3a, 3b, 3c, 3d. Sand exhibited low values in the lower (south) field portion, in exchange for high values in the upper (north) portion (Figure 3a). Furthermore, sand variability depicted inverse spatial trends to silt, clay, and CEC (figure 3b, 3c, and 3d, respectively). Silt, clay, and CEC values exhibited similar trends, showing high values in the south and low values in the north side of the field. Therefore, silt, clay, and CEC displayed a pattern similar to spatio-temporal yield (Figure 2a, 2b, 2c, 2d, 2e, 2f), whereas sand displayed a pattern in the opposite direction.

Figure **3**

Quality control of spatio-temporal YSCs

Significant correlations were evidenced between soil properties and the spatio-temporal yield data (Table 3). The sand content showed negative correlations with silt and clay, CEC, and spatio-temporal yield data (except for SF 2011). The silt and clay contents showed a positive correlation with each other and CEC, and they had positive correlations with crop yields, except for SF 2011. The CEC was positively correlated with single and multiple crop yields, except for SF 2011 and BW 2014. Additionally, high correlations were evidenced between spatio-temporal yields over single and multiple years: DW 2010, CO 2013 and BW 2014 yields showed the strongest relationship with multiple crop yield (r = 0.97** all) followed by BW 2012 (r = 0.78**) and SF 2011 (r = 0.73**).

Table **3**

Classification of stable soil physico-chemical properties within the three spatio-temporal yields classes depicted statistical differences of soil properties (Table 4).

Table **4**

The lowest mean value of sand (47.9 %) was associated with the HYS class, resulting in maximum yield over multiple crops (YSCs). Higher sand content was found in LYS (56.8 %) and unstable class (57.4 %), which featured a similar but statistically different yield (80 % and 83 %, respectively). Conversely, silt, clay, and CEC had higher values in the HYS class, compared to LYS and unstable class.

Ambient conditions during the five cropping seasons

The balance of ambient moisture in the five crop seasons is reported in Table 5.

Table **5**

During DW 2010, the crop growing period from tillering to heading (initial to mid-season) received a surplus of 206 mm as P-ETc difference and was considered a wet period, whereas late-season (ripening stage) staged a 68 mm deficit. BW 2012 and 2014 also received enough precipitation from tillering to stem elongation (28 and 212 mm surplus in the two respective years), whereas a dry period occurred from heading to ripening in both years. It resulted in a respective deficit of 298 and 249 mm. Compared to winter cereals, spring dicots SF 2011 and CO 2013 suffered an increasing water deficit across growth stages. At ripening, a cumulated deficit of 433 and 219 mm was attained in the two respective crops.

The representation of temperature and precipitation during the five growth seasons according to Bagnouls and Gaussen (1953) exhibits a similar picture (Figures S3 and S4).

The stronger drought experienced by the spring dicots vs. autumn cereals reflected in a stronger variation of yield data (Table 1a). Standard deviation was 38% of the mean GY in both SF 2011 and CO 2013, whereas it was 31%, averagely, in DW 2010, BW 2012, and BW 2014.

Discussion

The geostatistical analysis of the five crop yields featured quite similar parameters, despite using two different semivariogram models (Table 1b). BW 2012 represents the only partial exception, having a far more extended range than the rest of crops, associated with less spatial dependence. However, negligible nugget or barely exceeding 25% of the total sill, as in the case of BW 2012, indicates high spatial continuity between data points. This is a circumstance strengthening the value of the spatial variability maps obtained through kriging interpolation.

In these maps, the differences among the four yield classes that are evidenced in individual crops (Figure 2a, 2b, 2c, 2d, 2e) are softened in the multiple crops (Figure 2f). Therefore, the multiple crops play a buffering role vs. single crops, meaning that operating with the former data is as a sounder basis for crop management decisions to be taken.

The three YSCs proposed by Blackmore (2000) set themselves one step beyond spatial variability maps, as they combine spatial and temporal variability into a single indicator. The unstable class is that deserving most attention, as it is an area with a potential for improving crop yields. In our case, this area covers almost one-fourth of the total field surface (Table 2). Additionally, the unstable class has a patchy distribution across the field, whereas the two stable classes, HYS and LYS, have a more consistent shape and distribution (Figure 2h). Lastly, the unstable and LYS classes denote an increase in sand content and a parallel decrease in silt and clay content, and CEC (Table 4). Hence it is sensed that sharper values in soil properties lead to fluctuation and depression of final yield, whereas more balanced values conduct to consistently higher crop yields (Table 4).

The ECa survey directs soil sampling towards field areas more prone to indicate variations in soil properties, in contrast to regular grid sampling (Corwin et al. 2003). In our case, it is perceived that a higher density of sampling points was placed in the upper field portion (Figure 1), where the multiple-year data indicate systematic yield loss vs. the rest of the field (Figure 2f). Therefore, the ECa survey was shown able to predict soil constraints for plant growth. However, sampling and analysis were needed to detect the underlying causes, as premise for taking decisions to deal with constraints.

Overall, the mean values of spatial soil properties across the three YSCs show considerable differences and align with the multiple year yield map (Figure 2h). The considerable variations of crop yield across the whole field were quite well correlated with the variations of soil properties (Table 3); SF 2011 was a partial exception, but CO 2013, the other spring sown crop, behaved as the three winter wheat crops (DW 2010, BW 2012 and 2014). The general good correlations between crop yield and soil properties are in accordance with the findings of Corwin et al. (2003). It is evinced from their work and ours how much it is important to understand the causes of yield variation through soil factors that are expected to contribute to crop productivity.

Temporal stability is seen as a relevant property in multiple crops across multiple years. The unstable is made a class of its own in the YSC system (Blackmore 2000), to account for fluctuations which are due to crop type, weather, and undefined factors interacting with them (Figure 2g). We believe that this field portion that gave a slightly higher yield (83 %) than the LYS class (80 %) (Table 4), averagely, may require separate cultivation practices, depending on in-season weather conditions during the specific crop season. The unstable class was characterized by similar values of soil properties as the LYS class (Table 4), indicating that these levels of soil properties are prone to reduce crop yield. Therefore, the unstabilizing effect associated with these properties is responsible for reducing crop yield in areas that could potentially give a high yield. Separate cultivation practices aimed at reducing the negative effects of soil constraints in such areas should provide a gain in crop yields.

The weather pattern during the five growing seasons (Table 5, Figures S3 and S4) provides some clues to understanding why some field areas gave higher yield than others, and why some other areas behaved differently over time. The five rainfed crops were exposed to irregular weather, and the erratic pattern of water availability is acknowledged as one of the main determinants of crop yield and its variability (Kang et al. 2009; Kukal and Irmak 2018). Yield losses consequential to drought are commonly reported in the literature for wheat (Karim et al. 2000; Mirzaei et al. 2011), as well as sunflower (Nel et al. 2001) and coriander (Unlukara et al. 2016). However, the effect of ambient moisture that we noticed on yield spatial variability cannot be ascertained in small plot experiments and is relatively novel in the literature.

Additionally, our study suggests that, under favorable weather in a specific year, unstable field zones could be managed as high yielding ones, i.e. supplying a non-limiting amount of inputs to harness the favourable conditions conducive to high yield. Conversely, under unfavourable weather, savings could be made to avoid inefficient use of crop inputs.

In other words, while the stable yield zones of a field should be managed by strategic planning, the unstable zones shall better be managed by tactical approach, e.g., based on crop growth status and soil moisture conditions, which are a key factors for final yield in many agricultural areas around the world. Therefore, it is of paramount importance for the farmers to monitor their crop and receive timely we ather information for alternative decisions to be taken (Basso et al. 2011).

One last point concerns the management of fields that become larger and larger by merging previously separated fields, under the urge to increase the efficiency in agricultural practice. In the surveyed case, three consecutive fields, each approximately 200 m long in the north-south axis, were combined into a single field approximately 600 m long in 2006 (Figure S2). The result is that the northern third, which was planted with deep rooted tree crops, is scarcely productive, once converted to annual crops: in the multiple year average, a relative yield of 76 % can be calculated for the upper third, compared to 104 % and 124 % for the central and lower third.

There is no univocal answer to the dilemma whether to pursue the enlargement of crop fields, to the expenses of crop advocacy, or save advocacy, to the expenses of efficiency. In the former case, the assessment of the causes for low productivity in a field portion provides the grounds for applying the most suited crop husbandry in a site specific manner.

Conclusions

Site-specific zones are the basis in precision agriculture by understanding where variable crop inputs are needed, based on the spatial and temporal variability of field characteristics. This paper defines the concept of classified zones by delineating the potential yield stability classes based on spatio-temporal maps over a five-year series of yields obtained with different crops.

It is evinced that the field areas featuring unstable yield across years should be managed by considering the in-season weather information to predict whether the unstable field part will behave as high yielding or low yielding in a specific year. This will provide farmers with valuable support to decide the appropriate level of crop intensity, e.g., fertilizers or water supply, in a site-specific way.

Our work concludes that multi-year yield stability classes are a more practical and cost-effective approach than uniform management, as they set the premise for variable inputs to optimize crop productivity. Based on yield stability classes, strategic and tactical decisions must be taken in different field areas, depending on the spatial and temporal profile of productivity owned by these areas.

However, despite encouraging results based on a five-year data from a mixed cropping system, it is quite likely that the surrounding conditions play a relevant role in each specific case. This makes the approach described in this work reproducible, not simply generally valid, in different crop conditions.

Acknowledgements, The Agrisfera Cooperative is kindly acknowledged for the support during the field experiment.

In accordance with Taylor & Francis policy and my ethical obligation as a researcher, I am reporting that this research did not receive any specific grant from funding agencies in the public, commercial, or not-for-profit sectors.

Table 1. Descriptive statistics of (1a) and semivariogram analysis (1b) of relative yields (average = 100) over the five years

1a

Crop year	Min.	Max.	SD	Kurtosis	Skewness	K-S
DW 2010	13	156	29	-0.1	-0.6	**
SF 2011	12	190	38	-0.7	0.2	**
BW 2012	14	197	32	0.1	-0.1	**
CO 2013	19	181	38	-1.0	-0.3	**
BW 2014	21	178	33	-0.9	-0.2	**

1b

Crop year	Model	C_0	C_0+C	a (m)	C_0/(C_0+C) (%)	SpD
DW 2010	Stable	0.03	1.05	64	2.5	S
SF 2011	Exponential	0.01	1.01	38	1.0	S
BW 2012	Exponential	0.31	1.17	121	26.5	M
CO 2013	Stable	0.13	0.96	66	13.5	S
BW 2014	Stable	0.00	0.92	51	0.0	S

DW, durum wheat; SF, sunflower; BW, bread wheat; CO, coriander. Min., minimum; Max., maximum; SD, standard deviation; K-S, Kolmogorov-Smirnov test for normal distribution; **, significant at $P \leq 0.01$. C_0, nugget; C, partial sill; C_0+C, sill; a, range; $C_0/(C_0 + C)$, nugget to sill ratio; SpD, spatial dependence; S, strong; M, moderate; MAE, mean absolute error.

Table 2. Relative yield (average = 100) and CV data in spatio-temporal and yield stability classes.

Variables	**Relative yield or CV**	**Yield or CV classes**	**Grid points**	Area (%)
DW 2010	13-61	VL	134	11.6
	62-95	ML	317	27.4
	96-116	MH	301	26
	117-156	VY	404	35
SF 2011	12-61	VL	161	13.9
	62-95	ML	439	38
	96-134	MH	293	25.3
	135-190	VY	263	22.8
BW 2012	14-67	VL	176	15.2
	68-99	ML	374	32.4
	100-138	MH	506	43.8
	139-197	VY	100	8.6
CO 2013	19-60	VL	213	18.4
	61-99	ML	323	27.9
	100-131	MH	335	29
	132-181	VY	285	24.7
BW 2014	21-64	VL	176	15.2
	65-99	ML	387	33.5
	100-127	MH	304	26.3
	128-178	VY	289	25
Spatial map	27-66	VL	135	11.7
	67-99	ML	402	34.8
	100-120	MH	325	28.1
	121-148	VY	294	25.4
Temporal map (CV data)	2-14	Highly stable	334	28.9
	14-22	Medium stable	310	26.8
	22-30	Lowly stable	235	20.3
	30-73	Unstable	277	24
Yield stability classes		HYS	527	46
		LYS	352	30
		Unstable	277	24

DW, durum wheat; SF, sunflower; BW, bread wheat; CO, coriander; CV., coefficient of variation; VL, very low; ML, medium-low; MH, medium-high; VH, very high; HYS, high yielding and stable; LYS, low yielding and stable.

Table 3. Pearson correlations (r) between relevant soil properties and spatio-temporal relative yields in single and multiple crops.

Traits	Sand	Silt	Clay	CEC	DW 2010	SF 2011	BW 2012	CO 2013	BW 2014
Silt	-1.00**								
Clay	-0.96**	0.93**							
CEC	-0.91**	0.90**	0.91**						
DW 2010	-0.58**	0.59**	0.50*	0.52*					
SF 2011	-0.40	0.40	0.36	0.35	0.61**				
BW 2012	-0.63**	0.63**	0.57**	0.56**	0.72**	0.36			
CO 2013	-0.54*	0.57**	0.41	0.46*	0.96**	0.61**	0.72**		
BW 2014	-0.47*	0.49*	0.39	0.35	0.94**	0.68**	0.69**	0.94**	
Multiple crops	-0.58**	0.60**	0.49*	0.50*	0.97**	0.73**	0.78**	0.97**	0.97**

* and ** indicate r values significant at $P \leq 0.05$ and $P \leq 0.01$, respectively (n = 20).

Table 4. Statistical differences in soil properties and spatio-temporal relative yield among the three YSCs.

Variables	**YSCs**	**Data points**	**Mean**	**Min**	**Max**	**SD**
% sand	HYS	527	47.9 b	34.0	73.4	10.6
	LYS	352	56.8 a	33.6	75.6	10.6
	Unstable	277	57.4 a	37.1	73.5	9.4
% silt	HYS	527	40.2 a	20.0	50.6	8.2
	LYS	352	32.8 b	17.5	52.4	8.5
	Unstable	277	32.3 b	19.6	48.4	7.4
% clay	HYS	527	11.9 a	6.1	16.9	2.5
	LYS	352	10.4 b	6.2	15.0	2.3
	Unstable	277	10.4 b	6.3	14.8	2.1
CEC ($cmol_+$/kg)	HYS	527	10.8 a	7.6	13.4	1.1
	LYS	352	10.0 b	6.7	13.4	1.5
	Unstable	277	10.0 b	6.6	12.7	1.2
Rel. yield (multiple crops)	HYS	527	122 a	100	148	11.5
	LYS	352	80 c	27	100	15.4
	Unstable	277	83 b	29	136	26.4

YSCs, yield stability classes; HYS, high yielding and stable; LYS, low yielding and stable; SD, standard deviation.

Different letters indicate significantly different mean values (LSD test at $P \leq 0.05$).

Table 5. Weather conditions during the five crop seasons.

Crop and year	Growth period	Time (days)	P (mm)	ETc (mm)	P-ETc (mm)	Moisture condition
DW 2010	Ini	24	17	9	8	Wet
	Dev	65	180	26	154	Wet
	Mid	100	265	221	44	Wet
	Late	64	127	195	-68	Dry
SF 2011	Ini	35	31	41	-10	Dry
	Dev	40	29	142	-113	Dry
	Mid	50	67	278	-211	Dry
	Late	30	2	101	-99	Dry
BW 2012	Ini	19	35	10	25	Wet
	Dev	68	43	40	3	Wet
	Mid	116	77	245	-168	Dry
	Late	58	50	180	-130	Dry
CO 2013	Ini	20	22	23	-1	Dry
	Dev	30	36	83	-47	Dry
	Mid	25	5	141	-136	Dry
	Late	15	17	52	-35	Dry
BW 2014	Ini	44	96	13	83	Wet
	Dev	74	188	59	129	Wet
	Mid	79	86	273	-187	Dry
	Late	43	77	139	-62	Dry

DW, durum wheat; SF, sunflower; BW, bread wheat; CO, coriander; CV., coefficient of variation; P, precipitation; ETc, crop evapotranspiration; Ini, Initial; Dev, crop development; Mid, mid-season; Late, late-season.

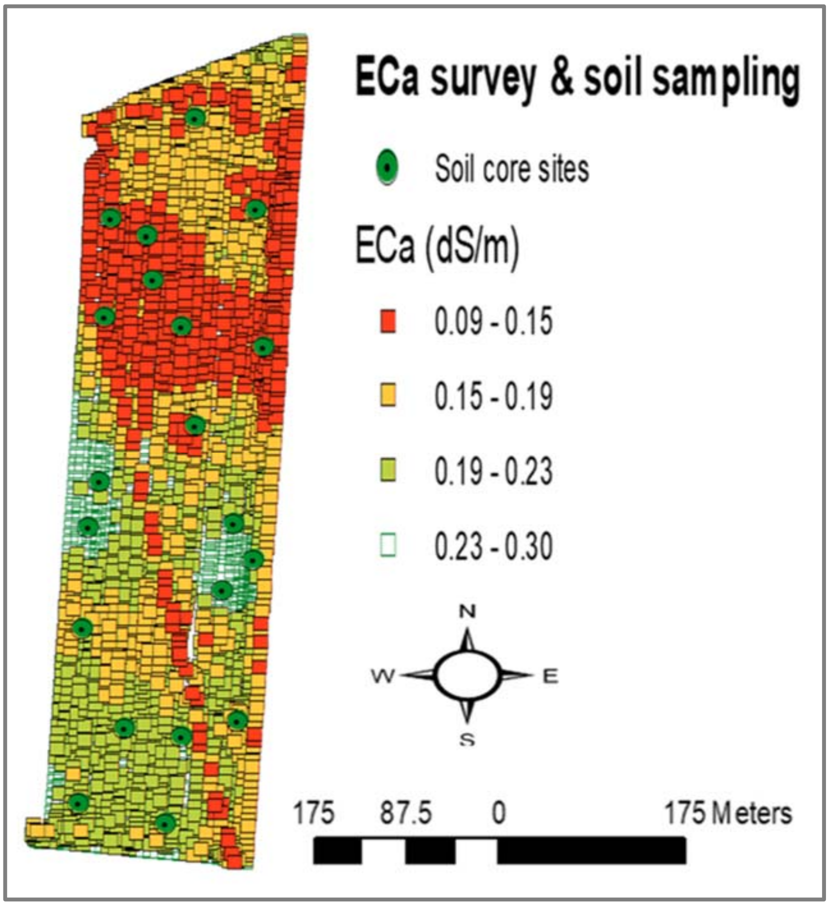

Figure 1. Map of the ECa distribution; green circles indicate the 20 soil sampling positions.

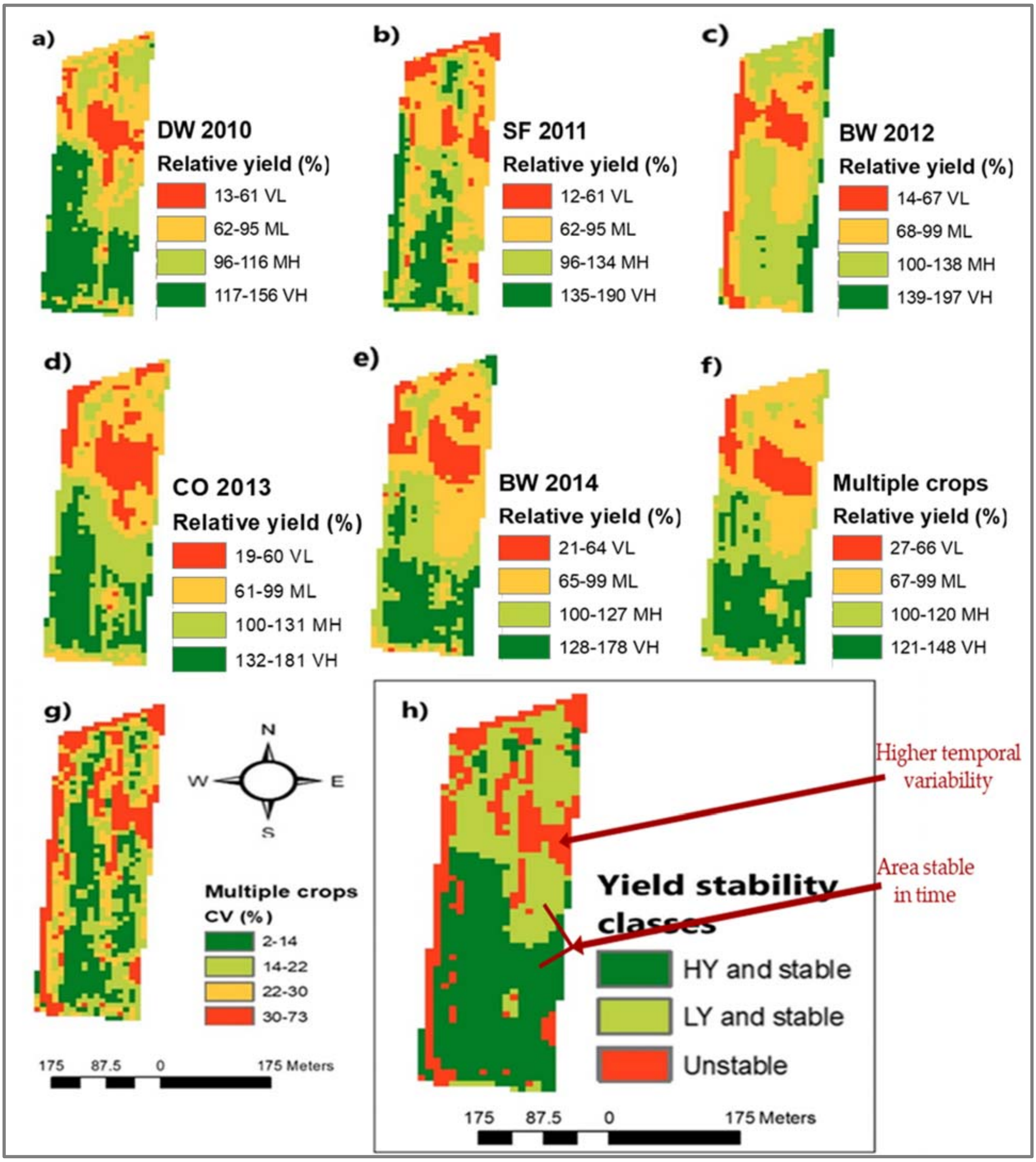

Figure 2. Consolidated spatio-temporal yield maps: VL, very low; ML, medium-low; MH, medium-high; VH, very high; 2a, spatial variability map of DW 2010; 2b, spatial variability map of SF 2011; 2c, spatial variability map of BW 2012; 2d, spatial variability map of CO 2013; 2e, spatial variability map of BW 2014; 2f, spatial variability map over 5 years' multiple crops; 2g,

temporal variability map over 5 years' multiple crops; 2h, yield stability classes over spatio-temporal variability over 5 years' multiple crops.

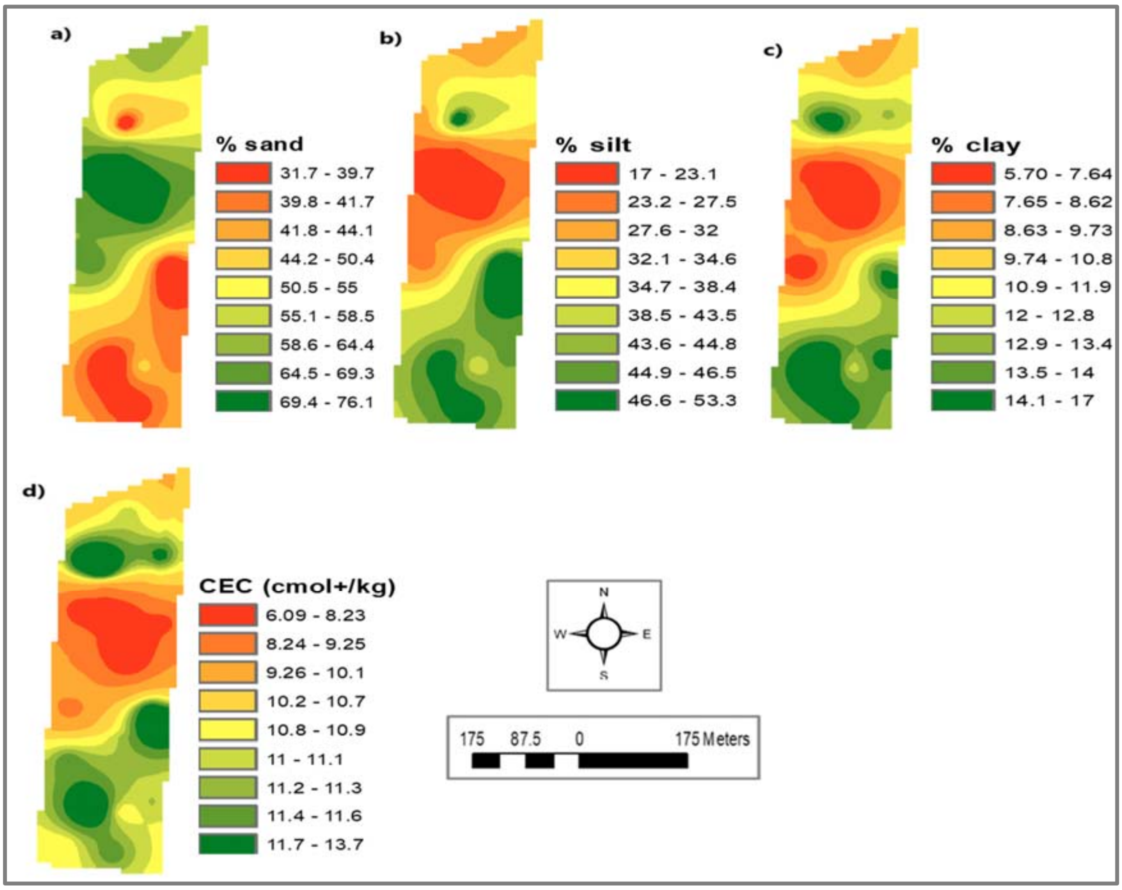

Figure 3a, 3b, 3c, 3d. Spatial variability maps of soil properties.

References

Ali A, Martelli R, Lupia F, Barbanti L. 2019. Assessing multiple years' spatial variability of crop yields using satellite vegetation indices. Remote Sens. 11(20):2384. https://doi.org/10.3390/rs11202384

Allen RG, Pereira LS, Raes D, Smith M. 1998. Crop evapotranspiration-Guidelines for computing crop water requirements-FAO Irrigation and drainage. FAO, Rome. Report No.: 56; D05109.

Asfaw A, Simane B, Hassen A, Bantider A. 2018. Variability and time series trend analysis of rainfall and temperature in northcentral Ethiopia: A case study in Woleka sub-basin. Weather Clim Extremes. 19:29-41.

Bagnouls F, Gaussen H. 1953. Saison sèche et indice xérothermique. Bull Soc His Nat Toulouse. 88:193-239.

Basso B, Dobrowolski J, McKay C. 2017. From the dust bowl to drones to big data: the next revolution in agriculture. Georget J Int Aff. 18(3):158–165.

Basso B, Ritchie JT, Cammarano D, Sartori L. 2011. A strategic and tactical management approach to select optimal N fertilizer rates for wheat in a spatially variable field. Eur J Agro. 35(4):215-222.

Bhunia GS, Shit PK, Maiti R. 2018. Comparison of GIS-based interpolation methods for spatial distribution of soil organic carbon (SOC). J Saudi Soc Agric Sci. 17(2):114-126.

Blackmore S. 2000. The interpretation of trends from multiple yield maps. Comput Electron Agric. 26(1):37-51.

Blackmore S, Godwin RJ, Fountas S. 2003. The analysis of spatial and temporal trends in yield map data over six years. Biosyst Eng. 84(4):455-466.

Bullock DS, Bullock DG. 2000. Economic optimality of input application rates in precision farming. Precis Agric. 2(1):71-101.

Cambardella CA, Moorman TB, Parkin TB, Karlen DL, Novak JM, Turco RF, Konopka AE. 1994. Field-scale variability of soil properties in central Iowa soils. Soil Sci Soc Am J. 58(5):1501-1511.

Ciesielski H, Sterckeman T. 1997. Determination of cation exchange capacity and exchangeable cations in soils by means of cobalt hexamine trichloride. Effects of experimental conditions. Agronomie. 17:1–7.

Corwin DL, Lesch SM. 2003. Application of soil electrical conductivity to precision agriculture. Agron J. 95(3): 455-471.

Corwin DL, Lesch SM. 2005. Characterizing soil spatial variability with apparent soil electrical conductivity: I. Survey protocols. Comput Electron Agric. 46(1-3):103-133.

Corwin DL, Lesch SM, Shouse PJ, Soppe R, Ayars JE. 2003. Identifying soil properties that influence cotton yield using soil sampling directed by apparent soil electrical conductivity. Agron J. 95(2):352-364.

Cuculeanu V, Tuinea P, Bălteanu D. 2002. Climate change impacts in Romania: Vulnerability and adaptation options. GeoJournal, 57(3):203-209.

Da Silva JM. 2006. Analysis of the spatial and temporal variability of irrigated maize yield. Biosyst Eng. 94(3):337-349.

Daniel S, Gabiri G, Kirimi F, Glasner B, Näschen K, Leemhuis C, Steinbach S, Mtei K. 2017. Spatial distribution of soil hydrological properties in the Kilombero floodplain, Tanzania. Hydrology. 4:57.

Fraisse CW, Sudduth KA, Kitchen NR, Fridgen J. 1999. Use of unsupervised clustering algorithms for delineating within-field management zones. St. Joseph: American Society of Agricultural Engineers.

Gee GW, Bauder JW, Klute A. 1986. Methods of soil analysis, part 1, physical and mineralogical methods. Soil Sci Soc of Am, Am Soc Agro.

Iizumi T, Ramankutty N. 2015. How do weather and climate influence cropping area and intensity? Glob Food Sec. 4:46-50.

Kang Y, Khan S, Ma X. 2009. Climate change impacts on crop yield, crop water productivity and food security–A review. Prog Nat Sci. 19(12):1665-1674.

Karim MA, Hamid A, Rahman S. 2000. Grain growth and yield performance of wheat under subtropical conditions: II. Effect of water stress at reproductive stage. Cereal Res Commun. 28(1-2):101-107.

Kravchenko A, Bullock DG. 1999. A comparative study of interpolation methods for mapping soil properties. Agron J. 91(3):393-400.

Kukal MS, Irmak S. 2018. Climate-driven crop yield and yield variability and climate change impacts on the US great plains agricultural production. Sci Rep. 8(1): 3450.

Lark RM, Stafford JV. 1996. Classification as a first step in the interpretation of temporal and spatial variability of crop yield. Asp Appl Biol. 46:139–142.

Lesch SM, Rhoades JD, Corwin DL. 2000. ESAP-95 Version 2.01 R: User manual and tutorial guide: Research Rpt. 146. Riverside (USA): USDA-ARS Salinity Laboratory.

Li Y, Shi Z, Wu CF, Li HY, Li F. 2008. Determination of potential management zones from soil electrical conductivity, yield and crop data. J Zhejiang Univ Sci B. 9(1):68-76.

Loeppert RH, Suarez DL. 1996. Carbonate and gypsum. Methods of Soil Analysis: Part 3 Chemical Methods. Vol.5. p. 437-474.

Maestrini B, Basso B. 2018. Drivers of within-field spatial and temporal variability of crop yield across the US Midwest. Sci Rep. 8(1):1-9.

Mariani L, Ferrante A. 2017. Agronomic management for enhancing plant tolerance to abiotic stresses—drought, salinity, hypoxia, and lodging. Horticulturae. *3*(4):52.

Metzger MJ, Bunce RGH, Jongman RH, Mücher CA, Watkins JW. 2005. A climatic stratification of the environment of Europe. Glob Ecol Biogeogr. 14(6):549-563.

Mirzaei A, Naseri R, Soleimani R. 2011. Response of different growth stages of wheat to moisture tension in a semiarid land. World Appl Sci J. 12(1):83-89.

Mohsenipour M, Shahid S, Chung ES, Wang XJ. 2018. Changing pattern of droughts during cropping seasons of Bangladesh. Water Resour Manag. 32(5):1555-1568.

Moral FJ, Terrón JM, Da Silva JM. 2010. Delineation of management zones using mobile measurements of soil apparent electrical conductivity and multivariate geostatistical techniques. Soil Tillage Res. 106(2):335-343.

Nel AA, Loubser HL, Hammes PS. 2001. The effect of water stress during grain filling on the yield and processing quality of sunflower seed. S Afr J Plant Soil. 18(3):114-117.

Olsen SR, Cole CV, Watandbe F, Dean L. 1954. Estimation of available phosphorus in soil by extraction with sodium bicarbonate. J Chem Inf Model. 53(9):1689-1699.

Orsini L, Remy JC. 1976. Utilisation du chlorure de cobaltihexamine pour la détermination simultanée de la capacité d'échange et des bases échangeables des sols. Sci Sol. 4:269-275.

Panneton B, Brouillard M. 2002. Use of fuzzy mapping to extract management zones from yield maps AIC 2002. CSAE/SCGR, Mansonville, QC, Canada.

Reza SK, Baruah U, Sarkar D, Das TH. 2010. Evaluation and comparison of ordinary kriging and inverse distance weighting methods for prediction of spatial variability of some chemical parameters of Dhalai district, Tripura. Agropedology. 20:38–48.

Scudiero E, Teatini P, Manoli G, Braga F, Skaggs T, Morari F. 2018. Workflow to establish time-specific zones in precision agriculture by spatiotemporal integration of plant and soil sensing data. Agronomy. 8(11):253.

Setia R, Gottschalk P, Smith P, Marschner P, Baldock J, Setia D, Smith J. 2013. Soil salinity decreases global soil organic carbon stocks. Sci Total Environ. 465:267-272.

Shiru M, Shahid S, Alias N, Chung ES. 2018. Trend analysis of droughts during crop growing seasons of Nigeria. Sustainability. 10(3):871.

Swindell JEG. 1997. Mapping the spatial variability in the yield potential of arable land through GIS analysis of sequential yield maps. Precision agriculture'97: papers presented at the first European Conference on Precision Agriculture, Warwick University Conference Centre; Sept 7-10; Oxford (UK).

Toshiro O. 2002. Classification Methods for Spatial Data Representation. Center for Advanced Spatial Analysis. London: University College London.

Unlukara A, Beyzi E, Ipek A, Gurbuz B. 2016. Effects of different water applications on yield and oil contents of autumn sown coriander (Coriandrum sativum L.). Turkish J Field Crop. 21(2):200-209.

Xiao Y, Gu X, Yin S, Shao J, Cui Y, Zhang Q, Niu Y. 2016. Geostatistical interpolation model selection based on ArcGIS and spatio-temporal variability analysis of groundwater level in piedmont plains, northwest China. SpringerPlus. 5:425. http://dx.doi.org/10.1186/s40064-016-2073-0.

Zandalinas SI, Mittler R, Balfagón D, Arbona V, Gómez-Cadenas A. 2018. Plant adaptations to the combination of drought and high temperatures. Physiol Plant. 162(1):2-12.